MATERIALS SCIENCE

General and selective deoxygenation by hydrogen using a reusable earth-abundant metal catalyst

T. Schwob[1], P. Kunnas[2], N. de Jonge[2,3], C. Papp[4], H.-P. Steinrück[4], R. Kempe[1]*

Chemoselective deoxygenation by hydrogen is particularly challenging but crucial for an efficient late-stage modification of functionality-laden fine chemicals, natural products, or pharmaceuticals and the economic upgrading of biomass-derived molecules into fuels and chemicals. We report here on a reusable earth-abundant metal catalyst that permits highly chemoselective deoxygenation using inexpensive hydrogen gas. Primary, secondary, and tertiary alcohols as well as alkyl and aryl ketones and aldehydes can be selectively deoxygenated, even when part of complex natural products, pharmaceuticals, or biomass-derived platform molecules. The catalyst tolerates many functional groups including hydrogenation-sensitive examples. It is efficient, easy to handle, and conveniently synthesized from a specific bimetallic coordination compound and commercially available charcoal. Selective, sustainable, and cost-efficient deoxygenation under industrially viable conditions seems feasible.

INTRODUCTION

The use of earth-abundant metals in catalytic reactions classically associated with noble metals might lead to a more sustainable chemistry and becomes especially attractive if unknown selectivity patterns are observed. Notable progress has been made recently concerning the use of homogeneous earth-abundant metal catalysts (*1*–*10*) for reactions customarily mediated by noble metals. However, the use of reusable nanostructured catalysts of such metals, broadly applicable in organic synthesis and essential for the production of fine and agrochemicals and pharmaceuticals, has been shown rarely (*11*–*14*).

An important problem in organic synthesis is the mild and selective defunctionalization of C—O bonds in the presence of other functional groups, such as in high-value fine chemicals, pharmaceuticals, or natural products (*15*). Such a selective deoxygenation method would allow the fine-tuning of highly functionalized molecules at the late stage of their synthesis. In addition, many biomass-derived platform molecules are highly oxidized, and the removal of surplus oxygen is key to their usability as fuels and bulk chemicals (*16*–*17*). Protocols based on the use of copper chromite catalysts play a distinct role in this area of research (*18*). C—O bond cleavage using inexpensive hydrogen gas (hydrodeoxygenation) is challenging but highly attractive for economic reasons. The hydrodeoxygenation of alcohols and carbonyl compounds in the presence of a large number of functional groups has been realized applying a homogeneous Ru catalyst (*19*). Tolerance of phenolic hydroxyl groups, aryl and alkyl ethers, olefins, fluorides, chlorides, a nitroarene, and an amide was observed. In addition, selective hydrodeoxygenation of diols has been demonstrated. A homogeneous or heterogeneous earth-abundant metal catalyst for the highly chemoselective hydrodeoxygenation of alcohols and carbonyl compounds has not yet been disclosed.

We report here on a nanostructured earth-abundant metal catalyst for the deoxygenation of various classes of chemical compounds using inexpensive hydrogen gas as the reducing agent. The process is highly chemoselective, and functional groups, easily reduced by hydrogen in the presence of conventional catalysts, remain unaffected. Halides (including reactive iodides), ethers (including thio- and benzyl ethers), an olefin, esters (including boronic esters), amides, carboxylic acids, phenols, and *N*-heterocycles are well tolerated. Furthermore, the selective removal of an OH group of a secondary or a tertiary alcohol in the presence of a primary alcohol was demonstrated. The catalyst system has a broad scope. Benzylic and purely aliphatic aldehydes, dialkyl, aryl-alkyl and diaryl ketones, as well as primary, secondary, and tertiary alcohols including purely aliphatic ones, complex natural products, pharmaceuticals, and biomass-derived platform molecules have been hydrodeoxygenated selectively. The catalyst is efficient and easy to handle, and its synthesis is simple and straightforward, starting from a specific Co-Ce bimetallic complex and commercially available charcoal. Elias *et al.* (*20*) introduced a synthetic route toward transition metal–substituted ceria nanoparticles, applying a solution-based processing and calcination of similar heterobimetallic complexes. The catalyst, synthesized from a Cu-Ce complex ($Cu_{0.1}Ce_{0.9}O_{2-x}$), showed high activity in the catalytic oxidation of carbon monoxide. Cerium is the most abundant element of the lanthanoids. It is more abundant in Earth's crust than the 3d metal cobalt (*21*). It is noteworthy to mention that inexpensive and easily available salts of these two metals, such as cobalt(II) acetate tetrahydrate and cerium(III) nitrate hexahydrate, are used for the preparation of the bimetallic complex. The catalyst proved stable over five consecutive runs without any remarkable decrease in product formation. Upscaling proceeds smoothly and in high yields (for example, small scale, 86%; large scale, 92%). We have recently introduced a variety of homogeneous earth-abundant catalysts (*22*–*28*) and reusable nanostructured catalysts for hydrogen storage (*29*) and organic reactions (*30*), including an earth-abundant metal catalyst (*31*).

RESULTS

Catalyst synthesis and characterization

The catalyst (Co-Ce/C) was synthesized in a convenient and practical two-step procedure. At first, commercially available activated charcoal (Norit CA1, Cabot Corporation) was impregnated with bimetallic complex **I**, followed by pyrolysis under a nitrogen atmosphere at 700°C and reduction (N_2/H_2, 90/10) at 550°C (Fig. 1A; Supplementary Materials for detailed information). Scanning electron microscopy

[1]Inorganic Chemistry II–Catalyst Design, University of Bayreuth, 95440 Bayreuth, Germany. [2]INM–Leibniz Institute for New Materials, Campus D2 2, 66123 Saarbrücken, Germany. [3]Department of Physics, Saarland University, Campus A5 1, 66123 Saarbrücken, Germany. [4]Physical Chemistry II, Department of Chemistry and Pharmacy, 91058 Erlangen, Germany.
*Corresponding author. Email: kempe@uni-bayreuth.de

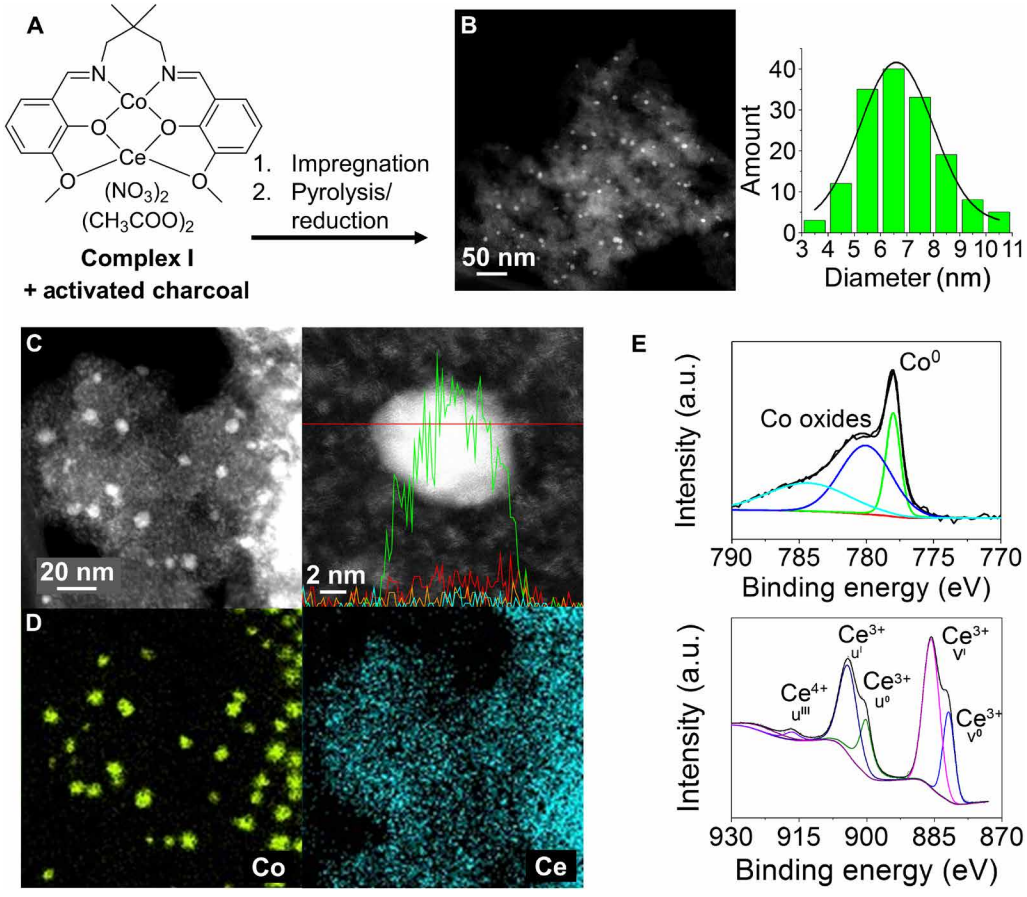

Fig. 1. Catalyst synthesis and characterization. (**A**) Synthesis of the catalyst by wet impregnation of commercially available charcoal with the bimetallic precursor complex **I**, followed by pyrolysis and reduction. (**B**) HAADF-STEM of the as-synthesized catalyst verifies the presence of homogeneously distributed metal nanoparticles with a mean diameter of 6.8 nm. (**C**) Detailed HAADF-STEM image in combination with EDX mapping. (**D**) EDX-based element mapping (Co, green; Ce, blue; O, red, P, orange) indicates that Co forms the nanoparticles and Ce is distributed over the whole carbon support. (**E**) XPS analysis confirms the presence of metallic cobalt (~20%) and cobalt oxide/hydroxide species (~80%). Ce is mainly present as Ce^{3+} (~ 90%) in addition to minor amounts of Ce^{4+} (~ 10%). a.u., arbitrary units.

(SEM) and energy-dispersive x-ray spectroscopy (EDX) indicated a homogeneous distribution of both metal species over the entire catalyst sample analyzed. The presence of phosphorous on the catalyst surface results from the chemically activated carbon support (fig. S1). High-angle annular dark-field scanning transmission electron microscopy (HAADF-STEM) provided evidence of the presence of two types of nanosized species homogeneously embedded in the matrix: nanoparticles with a mean diameter of 6.8 nm and smaller (~1 nm) structures (Fig. 1B). HAADF-STEM in combination with EDX mapping revealed that Co forms the 6.8-nm-diameter nanoparticles, while the element Ce is distributed in the matrix (Fig. 1, C and D, and fig. S2). HAADF-STEM combined with electron energy loss spectroscopy (EELS) indicated the presence of ~1-nm-sized cerium-rich structures in the vicinity of a Co nanoparticle (fig. S3). X-ray photoelectron spectroscopy (XPS) analysis of the Co $2p_{3/2}$ region confirmed the presence of metallic cobalt species (~20%) and oxides/hydroxides (~80%). Cerium is present as an oxide of predominantly Ce^{3+} (~90%) and small amounts of Ce^{4+} (~10%) (Fig. 1E and fig. S4), concluded from an analysis of the Ce $3d_{5/2}$ region. The catalyst features a specific surface area (Brunauer-Emmet-Teller) of 740 m^2/g and a 40% fraction of mesopores, which is in good accordance with the key figures of the pure carbon support (fig. S5). Inductively coupled plasma optical emission spectrometry (ICP-OES) revealed 3.6 weight % (wt %) Co and 7.3 wt % Ce in the as-synthesized catalyst sample.

Screening of reaction parameters

The hydrodeoxygenation of acetophenone was chosen to optimize the catalyst system and reaction conditions. A pyrolysis temperature of 700°C was found to be optimal, and the desired product ethylbenzene was obtained in 81% yield. The use of catalysts pyrolyzed at 600° or 800°C led to a distinct drop of product yields under the same reaction conditions (table S1). Methylcyclohexane emerged as the most suitable reaction solvent from a comparison of eight different solvents (table S2). We compared different supports and metal sources under identical reaction conditions to demonstrate the superiority of the bimetallic Co-Ce/C catalyst. Only the combination of TiO_2 with bimetallic complex **I** gave moderate yields of the desired product, while poor yields were achieved using CeO_2 and Al_2O_3 as support (Table 1, entries 1 to 4). When complex **I** was replaced by the common metal salts $Co(NO_3)_2$ and $Ce(NO_3)_3$, no ethylbenzene formation could be detected (Table 1, entry 6). To ensure the necessity of bimetallic complex **I**, the monometallic Co complex **II** (essentially complex **I** without Ce) and the monometallic Ce complex **III** (essentially complex **I** without Co) were used for the catalyst synthesis (fig. S6). Neither

Table 1. Catalyst screening.

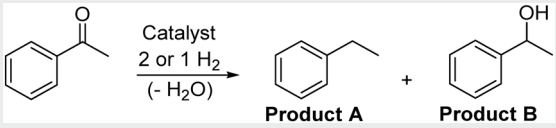

Entry	Metal source	Support	Yield (%)	
			Product A	Product B
1	Bimetallic complex **I**	TiO_2	62	27
2	Bimetallic complex **I**	CeO_2	15	69
3	Bimetallic complex **I**	γ-Al_2O_3	6	21
4	Bimetallic complex **I**	Activated charcoal	81	16
5*	Bimetallic complex **I**	Activated charcoal	98	—
6	$Co(NO_3)_2 + Ce(NO_3)_3$	Activated charcoal	—	18
7†	Monometallic complex **II**	Activated charcoal	—	10
8‡	Monometallic complex **III**	Activated charcoal	—	—
9	Monometallic complex **II** + **III**	Activated charcoal	32	51

Reaction conditions: 0.5 mmol of substrate, 15 mg of catalyst (1.8 mol % Co, 1.6 mol % Ce), 100°C, 4.0 MPa H_2, 3 ml of methylcyclohexane, 20 hours. *110°C reaction temperature; †1.8 mol % Co without Ce; ‡1.6 mol % Ce without Co. Yields were determined by GC and GC-MS using *n*-dodecane as an internal standard.

the use of complex **II**, **III** nor a combination of both led to comparable hydrodeoxygenation activities (Table 1, entries 7 to 9). In summary, the hydrodeoxygenation of acetophenone proceeded well, applying a catalyst prepared from bimetallic complex **I** and activated charcoal by pyrolysis at 700°C (3.6 wt % Co, 7.3 wt % Ce). A further optimization of the reaction conditions led to the following parameters: 0.5 mmol substrate, 15 mg of catalyst [1.8 mole percent (mol %) Co, 1.6 mol % Ce], 3 ml of methylcyclohexane, 4.0 MPa H_2, 20 hours. The reaction temperature was slightly increased to 110°C to lastly ensure maximum yields of the desired product (Table 1, entry 5).

Substrate scope

Having optimized the reaction conditions of the catalytic hydrodeoxygenation protocol, we explored the substrate scope. The product yields of the test reactions were determined by gas chromatography (GC) and GC–mass spectrometry (MS), and products were isolated for selected examples. The isolated yields are given in parentheses (Figs. 2 and 3).

First, we investigated the hydrodeoxygenation of aryl-alkyl ketones and related secondary alcohols (Fig. 2, top). The introduction of methyl and electron-rich methoxy substituents had no notable influence on the conversion, and the corresponding products were obtained in yields around 90% (Fig. 2, products **1b** and **1c**). The hydrodeoxygenation of halogenated substrates is more challenging since dehalogenation can take place. We expected an activation of these substrates by Brønsted or Lewis acids, as described in the literature for a variety of different reactions (*32*). To our delight, the reduction proceeded well, applying 10 mg of Amberlyst 15 as an additive (table S3). 4-Fluoro- or 4-chloro-acetophenone was smoothly converted, no dehalogenation was observed, and nearly quantitative yields were obtained (Fig. 2, products **1d** and **1g**). Product yields around 70% were observed for the sterically more demanding 2-chloroacetophenone and the corresponding 3-chloro–substituted derivative (Fig. 2, products **1e** and **1f**). Aryl bromide withstood the deoxygenation well as can be seen from the formation of **1h** in nearly 80% yield. Dehalogenation was observed in the case of aromatic ketones bearing aliphatic halide functionalities (4-chloro-1-phenylbutan-1-one), and no product formation could be detected. Further functional groups such as amines, esters, amides, thioethers, and ethers, as well as *N*-heterocycles or phenols were tolerated under reaction conditions (Fig. 2, products **1i** to **1p**). The performance of the catalyst was further evaluated on diaryl ketones. Benzophenone, for instance, was deoxygenated to afford diphenylmethane in 92% yield (Fig. 2, product **1r**). Fluorinated and chlorinated 1-phenylethanol derivatives could be deoxygenated as smoothly as the corresponding ketones. The desired products were obtained in yields higher than 80% (Fig. 2, products **1u** and **1v**). It is noteworthy that even the challenging iodo substituent of 1-(4-iodophenyl)ethanol resisted the deoxygenation conditions (Fig. 2, product **1w**).

The transformation of benzylic aldehydes and related primary alcohols required slightly harsher reaction conditions and higher catalyst loadings (130°C, 6.0 MPa, 6.1 mol % Co, 5.2 mol % Ce). But even then, the hydrodeoxygenation of halogenated substrates proceeded well when 5 mol % $Zn(OTf)_2$ was added (table S3). Substrates bearing electron-withdrawing or electron-donating moieties, such as halides, amides, heterocycles, and amino, hydroxy, and methoxy functionalities, were well tolerated (Fig. 2, products **2a** to **2j**, **2l**, and **2n** to **2q**). 4-Benzyloxybenzaldehyde was deoxygenated selectively to give benzyl-*p*-tolyl ether **2m** in excellent yield without a notable amount of hydrogenolytic ether cleavage (Fig. 2). The stability of boronic esters, which are common starting materials for cross-coupling reactions, is of special importance (Fig. 2, product **2k**).

We next examined the transformation of aliphatic alcohols and carbonyl compounds, tertiary alcohols, diols, biomass-derived substrates, and more complex organic molecules to further evaluate the scope of possible substrates (Fig. 3). Triphenylmethanol was easily

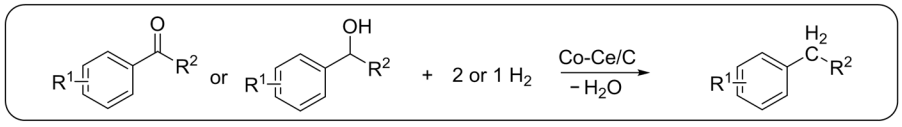

Ketones and secondary alcohols[a]

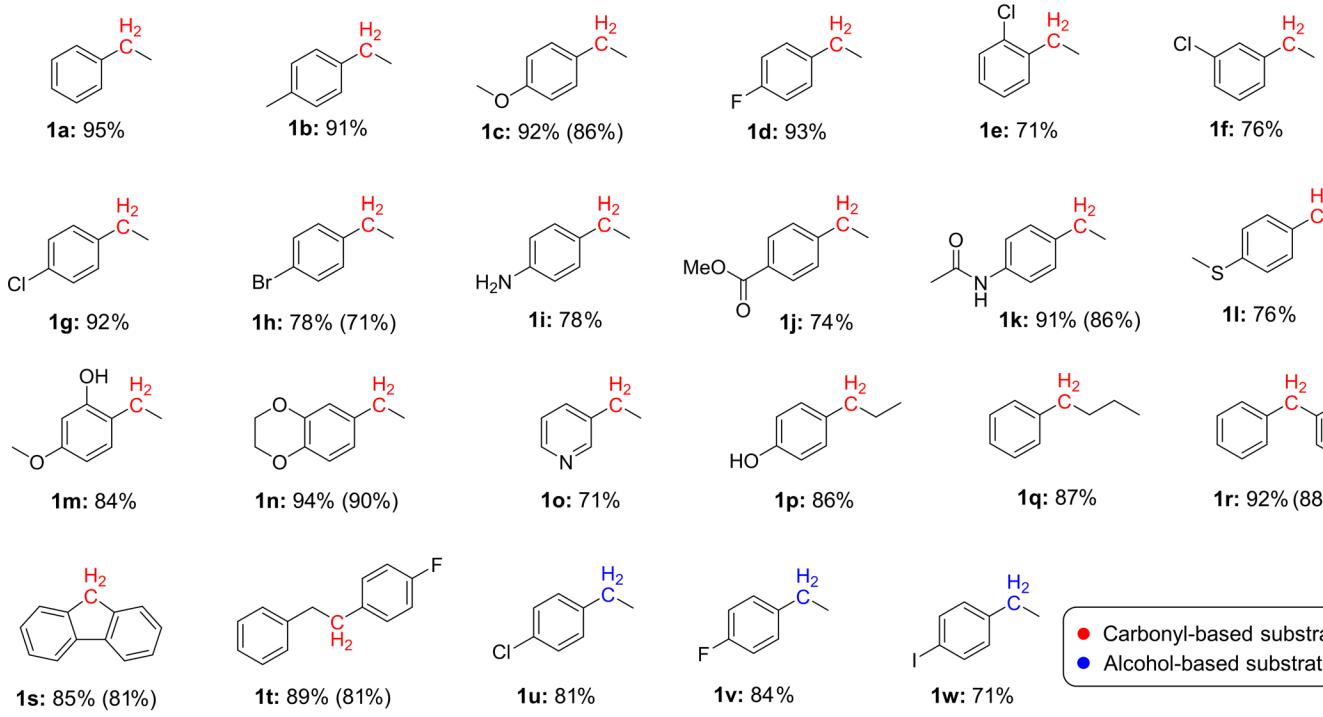

Aldehydes and primary alcohols[b]

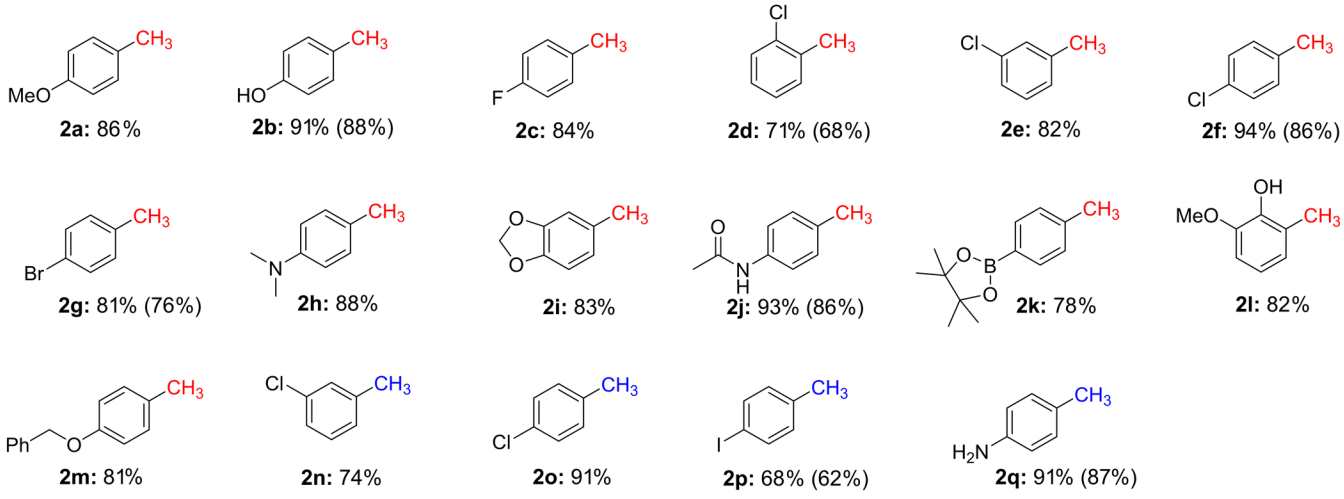

Fig. 2. Selective hydrodeoxygenation of alcohols and carbonyl compounds I. [a] Reaction conditions: 0.5 mmol substrate, 15 or 35 mg of catalyst (1.8 mol % Co and 1.6 mol % Ce, or 4.2 mol % Co and 3.7 mol % Ce, respectively), 110° to 130°C, 5.0 MPa H_2, 3 ml of methylcyclohexane, 20 hours (10 mg of Amberlyst 15 for halogenated substrates). [b] Reaction conditions: 0.5 mmol substrate, 50 mg of catalyst (6.1 mol % Co, 5.2 mol % Ce), 130°C, 6.0 MPa H_2, 3 ml of methylcyclohexane, 20 hours [5 mol % $Zn(OTf)_2$ for halogenated substrates]. Yields were determined by GC and GC-MS using *n*-dodecane as an internal standard. Isolated yields in parentheses.

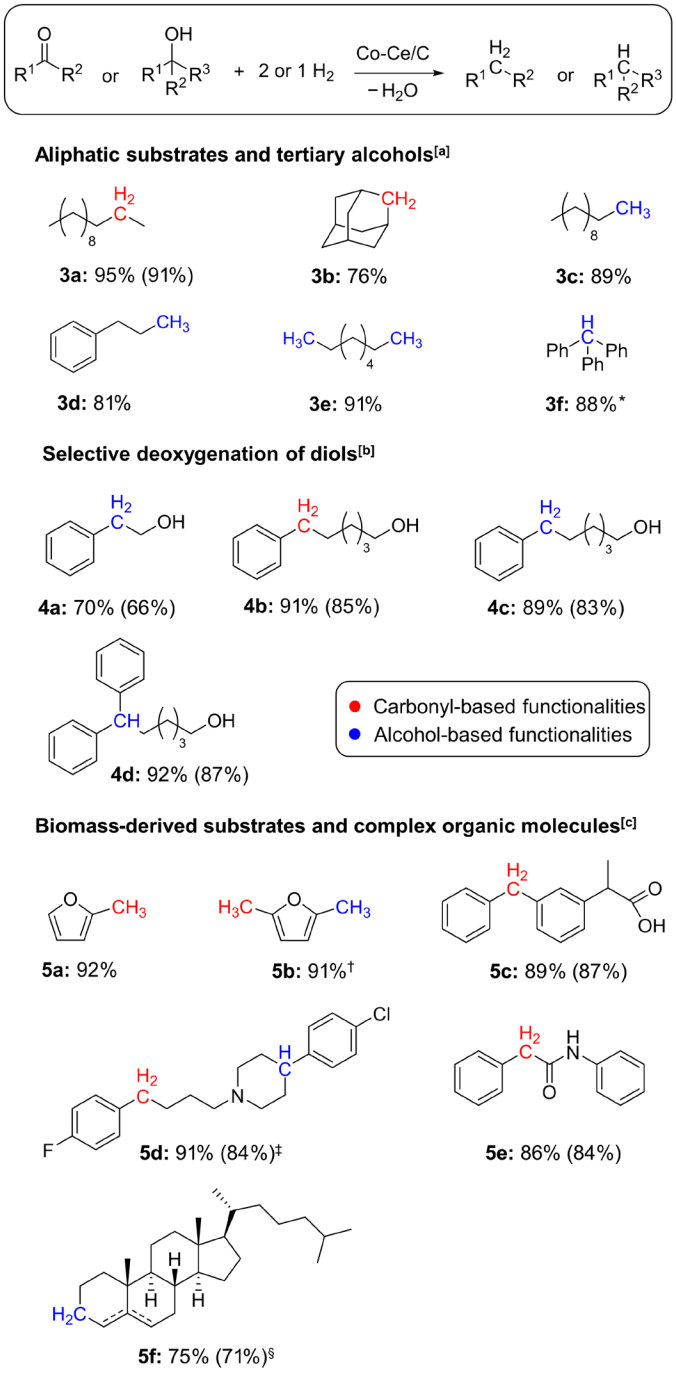

Fig. 3. Selective hydrodeoxygenation of alcohols and carbonyl compounds II. [a] Reaction conditions: 1.0 mmol substrate, 100 mg of catalyst (6.1 mol % Co, 5.2 mol % Ce), 160°C, 6.0 MPa H_2, 6 ml of methylcyclohexane, 20 mg of Amberlyst 15, 20 hours; *1 mmol substrate, 30 mg of catalyst (1.8 mol % Co, 1.6 mol % Ce), 110°C, 4.0 MPa H_2, 6 ml of methylcyclohexane, 20 hours, no additive. [b] Reaction conditions: 1.0 mmol substrate, 70 mg of catalyst (4.2 mol % Co, 3.7 mol % Ce), 130°C, 5.0 MPa H_2, 6 ml of ethanol, 20 hours. [c] Reaction conditions: 1.0 mmol substrate, 100 mg of catalyst (6.1 mol % Co, 5.2 mol % Ce), 160°C, 6.0 MPa H_2, 6 ml of methylcyclohexane, 20 hours; †diglyme was used as the solvent; ‡20 mg of Amberlyst 15 as additive; §5 mol % $Zn(OTf)_2$ as additive. Yields were determined by GC and GC-MS using *n*-dodecane as an internal standard. Isolated yields are given in parentheses.

reduced to triphenylmethane applying only 110°C reaction temperature, 4.0-MPa hydrogen pressure, and a catalyst loading of 1.8 mol % Co and 1.6 mol % Ce (Fig. 3, product **3f**). Hydrogenolysis of purely aliphatic compounds typically requires harsher reaction conditions and higher catalyst loadings. A variety of cyclic and linear substrates were deoxygenated in up to 91% yield (Fig. 3, products **3a** to **3e**). We expected the selective removal of only one OH group in diols due to the different reaction conditions needed to deoxygenate primary, secondary, and tertiary alcohols. A few diols were selectively reduced in up to 92% isolated yield (Fig. 3, products **4a**, **4c**, and **4d**). The preferred removal of a secondary or tertiary alcohol in the presence of a primary alcohol was observed. This selectivity is inverse to that observed in a Wolff-Kishner–based catalytic deoxygenation approach (*33*). Even a ketone could be deoxygenated in the presence of a primary alcohol (Fig. 3, product **4b**). The transformation of biomass-derived furfural and hydroymethyfurfural proceeded well (Fig. 3, products **5a** and **5b**) (*34*, *35*). In addition, a high selectivity (88%) toward the formation of 1,2-propanediol was observed in the deoxygenation of glycerol (table S4). The hydrodeoxygenation protocol may also be applied to more complex organic molecules (Fig. 3, bottom). Ketoprofen and haloperidol were deoxygenated to the respective products in up to 87% isolated yield (Fig. 3, products **5c** and **5d**). The reduction in a sterically demanding alpha-ketoamide was accomplished without any side product formation (Fig. 3, product **5e**). In the case of cholesterol, unexpectedly, we observed a chemoselectivity for carbonyl reduction over double-bond hydrogenation, and a mixture of olefin isomerization products was obtained in 71% isolated yield (Fig. 3, product **5f**).

Role of the metal components and oxidation states

Regarding the hydrodeoxygenation of acetophenone, we propose a hydrogenation-dehydration-hydrogenation pathway, as shown in Fig. 4 (*15*). Thirteen catalysts were synthesized and applied in the individual reaction steps to get a deeper insight into the role of the different metal components. The results are summarized in tables S5 to S7. The comparison demonstrates that only the catalyst synthesized from bimetallic complex **I** and activated charcoal can mediate all reaction steps. Even under mild conditions (90°C, 3.0 MPa H_2), nearly quantitative conversion of acetophenone was achieved and a product mixture of 1-phenlyethanol and ethylbenzene was detected (table S5, entry 4). Incomplete conversion was observed for the TiO_2- and CeO_2-supported catalysts (table S5, entries 1, 2). The catalyst, which was synthesized from the monometallic Co-salen complex and CeO_2, showed a high selectivity toward 1-phenylethanol formation, but no hydrodeoxygenation was observed (table S5, entry 6). This indicates the importance of Ce^{3+}/Ce^{4+} at the surface in the dehydration step. When 1-phenylethanol was used as the substrate (table S6), no product formation was detected applying the monometallic Co-salen complex on CeO_2 (Co/CeO_2 catalyst, table S6, entry 6). This indicates that Co on ceria is not an efficient hydrodeoxygenation catalyst under these mild conditions. By contrast, a nearly quantitative yield of ethylbenzene was observed for the Co-Ce/C catalyst under the same conditions (table S6, entry 4). No dehydration was observed applying the monometallic Co-salen and Ce-salen complexes, in combination with all support materials (table S6, entries 5 to 12), which demonstrates the necessity of both metal species in this reaction step. It is noteworthy that only trace amounts of styrene intermediate were observed, even at moderate conversion of the substrate, indicating a fast hydrogenation of the olefin intermediate (table S6,

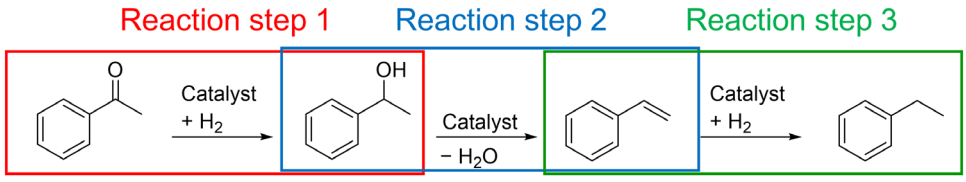

Fig. 4. Proposed reaction pathway regarding the hydrodeoxygenation of acetophenone.

entries 1 and 2). A catalyst screening regarding the hydrogenation of styrene revealed that all samples containing cobalt mediate the hydrogenation of the C—C double bond (table S7). Olefin hydrogenation activity could also be observed for catalysts, which did not show any product formation regarding the hydrogenation of the carbonyl functionality. Our catalyst synthesis leads to the formation of cobalt/cobalt oxide and Ce^{3+}/Ce^{4+} surfaces. This seems to be crucial for high activity in the dehydration of the alcohol intermediate under mild conditions. We next investigated the influence of the oxidation states of both metal species by preparing two modified catalysts. The first sample was oxidized (250°C, air, 1 hour), and the second sample was additionally reduced (550°C, N_2/H_2 90/10, 1 hour). Both catalysts were characterized by XPS analysis (fig. S8). After the oxidation process, no metallic cobalt was found on the catalyst surface (fig. S8A), while a subsequent treatment under reductive atmosphere led to the formation of metallic Co (fig. S8B). A comparison of the Ce 3d region of the oxidized and reduced catalyst sample showed no changes within the accuracy of the measurements. A majority of Ce^{3+} and small amounts of Ce^{4+} species were identified in both cases. The catalysts were applied in the individual reaction steps, and the results are summarized in tables S8 to S10. While the reduced catalyst can mediate all reaction steps (tables S8 to S10, entry 2), the oxidized sample showed no activity in the hydrogenation of the carbonyl and olefin functionality (tables S8 and S10, entry 1). This indicates the necessity of metallic cobalt species in the hydrogenation steps. The oxidized catalyst is active in the dehydration of 1-phenylethanol (88% conversion), and styrene was obtained in 41% yield (table S9, entry 1). However, a high amount of side product formation was observed, resulting from a reaction of styrene and alcohol intermediates (ether formation). A fast hydrogenation of the double-bond intermediate seems to be necessary to prevent the formation of these unwanted side products.

Recyclability and upscaling

The hydrodeoxygenation of acetophenone was chosen to demonstrate the recyclability of the catalyst, which was reused in five consecutive runs without any noticeable reduction of catalytic activity (fig. S9). ICP-OES revealed a very low amount of leaching of both metal species during a catalytic cycle (0.08% Co and 0.09% Ce regarding the initial metal content). The reused catalyst was characterized by a combination of HAADF, EELS, and XPS measurements. No notable growth of the cobalt nanoparticles (~6 nm) was observed. Cerium is still homogenously distributed in the matrix; however, some larger agglomerates (~7 nm) were also found (fig. S10, A to D). XPS analysis of the Co $2p_{3/2}$ indicates a slight decrease in the amount of metallic cobalt species on the catalyst surface after the fifth run. A comparison of the Ce 3d region of the as-synthesized and reused catalyst showed no change within the accuracy of the measurement. The surface of the reused catalyst consists mainly of Ce^{3+} with small amounts of Ce^{4+} (fig. S10, E and F). An upscaling of the reaction had no notable influence on the catalytic results. 4-Acetamidoacetophenone (10 mmol) was deoxygenated smoothly to afford the desired product in virtually quantitative yield (table S11).

CONCLUSION

Cost-efficient and selective late-stage deoxygenation of fine chemicals, natural products, and pharmaceuticals under industrially viable and scalable conditions seems feasible now. The protocol is especially sustainable since a reusable earth-abundant metal catalyst is used. Our work may inspire others to develop reusable and nanostructured earth-abundant metal catalysts for complex organic transformations in which the tolerance of functional groups has been a key challenge so far (*36*).

MATERIALS AND METHODS

Catalyst preparation

An amount of 300 mg of activated charcoal was added to a solution of 164 mg of (M = 809.58 g mol^{-1}, 0.2026 mmol) complex **I** in 3 ml of acetonitrile, and the suspension was stirred at 95°C. After evaporation of the solvent, the sample was pyrolyzed under a nitrogen atmosphere at 700°C followed by reduction at 550°C (N_2/H_2, 90/10). The catalysts used for the screening reactions were synthesized using equivalent amounts of monometallic complexes or metal salts.

General catalytic procedures

A 5-ml Teflon reaction vial was charged with a magnetic stirring bar, 0.5 mmol substrate, 3 ml of methylcyclohexane, and 15 or 35 mg of catalyst (1.8 mol % Co and 1.6 mol % Ce, or 4.2 mol % Co and 3.7 mol % Ce, respectively). An amount of 10 mg of Amberlyst 15 for halogenated ketones and secondary alcohols and 5 mol % $Zn(OTf)_2$ for halogenated aldehydes and primary alcohols were used as additives. The vial was placed in a 300-ml high-pressure autoclave (Parr Instruments), and the autoclave was flushed three times with 2.0-MPa hydrogen. Afterward, the final pressure was applied, and the reaction was stirred at the desired temperature for 20 hours (reaction conditions vary depending on the substrate). After completion of the reaction time, the autoclave was cooled to room temperature and the hydrogen was released. Quantitative GC analysis was accomplished using *n*-dodecane as an internal standard.

SUPPLEMENTARY MATERIALS

Supplementary material for this article is available at http://advances.sciencemag.org/cgi/content/full/5/11/eaav3680/DC1

Supplementary Materials and Methods

Fig. S1. SEM in combination with EDX analysis of the activated charcoal support and the active catalyst system.

Fig. S2. Characterization of the active catalyst by HAADF-STEM analysis combined with energy-dispersed x-ray element maps.

Fig. S3. HAADF-STEM combined with EELS.

Fig. S4. XPS analysis of the Co-Ce catalyst.
Fig. S5. Nitrogen physisorption measurements of the catalyst in comparison to the pure carbon support.
Fig. S6. Structures of the different salen complexes.
Fig. S7. Proposed reaction pathway for the hydrodeoxygenation of acetophenone.
Fig. S8. XPS analysis of the different catalyst samples.
Fig. S9. Recycling study.
Fig. S10. Catalyst characterization after the fifth run.
Table S1. Screening of reaction parameters—pyrolysis temperature.
Table S2. Screening of reaction parameters—solvent.
Table S3. Screening of reaction parameters—additive.
Table S4. Hydrodeoxygenation of glycerol—screening of reaction temperature.
Table S5. Catalyst screening for the hydrogenation of acetophenone.
Table S6. Catalyst screening for the dehydration/hydrogenation of 1-phenylethanol.
Table S7. Catalyst screening for the hydrogenation of styrene.
Table S8. Catalyst comparison—hydrogenation of acetophenone.
Table S9. Catalyst comparison—dehydration of 1-phenylethanol.
Table S10. Catalyst comparison—hydrogenation of styrene.
Table S11. Upscaling of the reaction.
Table S12. Solvent deoxygenation study.
Characterization of isolated products
NMR Spectra
References (*37*–*40*)

REFERENCES AND NOTES

1. A. Boddien, D. Mellmann, F. Gärtner, R. Jackstell, H. Junge, P. J. Dyson, G. Laurenczy, R. Ludwig, M. Beller, Efficient dehydrogenation of formic acid using an iron catalyst. *Science* **333**, 1733–1736 (2011).
2. A. M. Tondreau, C. C. Hojilla Atienza, K. J. Weller, S. A. Nye, K. M. Lewis, J. G. P. Delis, P. J. Chirik, Iron catalysts for selective anti-Markovnikov alkene hydrosilylation using tertiary silanes. *Science* **335**, 567–570 (2012).
3. W. Zuo, A. J. Lough, Y. F. Li, R. H. Morris, Amine(imine)diphosphine iron catalysts for asymmetric transfer hydrogenation of ketones and imines. *Science* **342**, 1080–1083 (2013).
4. M. R. Friedfeld, M. Shevlin, J. M. Hoyt, S. W. Krska, M. T. Tudge, P. J. Chirik, Cobalt precursors for high-throughput discovery of base metal asymmetric alkene hydrogenation catalysts. *Science* **342**, 1076–1080 (2013).
5. J. M. Hoyt, V. A. Schmidt, A. M. Tondreau, P. J. Chirik, Iron-catalyzed intermolecular [2+2] cycloadditions of unactivated alkenes. *Science* **349**, 960–963 (2015).
6. T. J. Korstanje, J. I. van der Vlugt, C. J. Elsevier, B. de Bruin, Hydrogenation of carboxylic acids with homogeneous cobalt catalyst. *Science* **350**, 298–302 (2015).
7. R. P. Yu, D. Hesk, N. Rivera, I. Pelczer, P. J. Chirik, Iron-catalysed tritiation of pharmaceuticals. *Nature* **529**, 195–199 (2016).
8. M. R. Friedfeld, H. Zhong, R. T. Ruck, M. Shevlin, P. J. Chirik, Cobalt-catalyzed asymmetric hydrogenation of enamides enabled by single-electron reduction. *Science* **360**, 888–893 (2018).
9. G. A. Filonenko, R. van Putten, E. J. M. Hensen, E. A. Pidko, Catalytic (de)hydrogenation promoted by non-precious metals – Co, Fe and Mn: Recent advances in an emerging field. *Chem. Soc. Rev.* **47**, 1459–1483 (2018).
10. F. Kallmeier, R. Kempe, Manganese complexes for (de)hydrogenation catalysis: A comparison to cobalt and iron catalysts. *Angew. Chem. Int. Ed.* **57**, 46–60 (2018).
11. R. V. Jagadeesh, A.-E. Surkus, H. Junge, M.-M. Pohl, J. Radnik, J. Rabeah, H. Huan, V. Schünemann, A. Brückner, M. Beller, Nanoscale Fe_2O_3-based catalysts for selective hydrogenation of nitroarenes to anilines. *Science* **342**, 1073–1076 (2013).
12. F. A. Westerhaus, R. V. Jagadeesh, G. Wienhöfer, M.-M. Pohl, J. Radnik, A.-E. Surkus, J. Rabeah, K. Junge, H. Junge, M. Nielsen, A. Brückner, M. Beller, Heterogenized cobalt oxide catalysts for nitroarene reduction by pyrolysis of molecularly defined complexes. *Nat. Chem.* **5**, 537–543 (2013).
13. R. V. Jagadeesh, K. Murugesan, A. S. Alshammari, H. Neumann, M.-M. Pohl, J. Radnik, M. Beller, MOF-derived cobalt nanoparticles catalyze a general synthesis of amines. *Science* **358**, 326–332 (2017).
14. T. Zhang, K. Manna, W. Lin, Metal–organic frameworks stabilize solution-inaccessible cobalt catalysts for highly efficient broad-scope organic transformations. *J. Am. Chem. Soc.* **138**, 3241–3249 (2016).
15. J. M. Herrmann, B. König, Reductive deoxygenation of alcohols: Catalytic methods beyond Barton–McCombie deoxygenation. *Eur. J. Org. Chem.* **2013**, 7017–7027 (2013).
16. J. N. Chheda, G. W. Huber, J. A. Dumesic, Liquid-phase catalytic processing of biomass-derived oxygenated hydrocarbons to fuels and chemicals. *Angew. Chem. Int. Ed.* **46**, 7164–7183 (2007).
17. R. A. Sheldon, Green and sustainable manufacture of chemicals from biomass: State of the art. *Green Chem.* **16**, 950–963 (2014).
18. A. Corma, S. Iborra, A. Velty, Chemical routes for the transformation of biomass into chemicals. *Chem. Rev.* **107**, 2411–2502 (2007).
19. N. Kalutharage, C. S. Yi, Scope and mechanistic analysis for chemoselective hydrogenolysis of carbonyl compounds catalyzed by a cationic ruthenium hydride complex with a tunable phenol ligand. *J. Am. Chem. Soc.* **137**, 11105–11114 (2015).
20. J. S. Elias, M. Risch, L. Giordano, A. N. Mansour, Y. Shao-Horn, Structure, bonding, and catalytic activity of monodisperse, transition-metal-substituted CeO_2 nanoparticles. *J. Am. Chem. Soc.* **136**, 17193–17200 (2014).
21. G. B. Haxel, J. B. Hedrick, G. J. Orris, Rare Earth Elements—Critical Resources for High Technology; https://pubs.usgs.gov/fs/2002/fs087-02/.
22. S. Rösler, J. Obenauf, R. Kempe, A highly active and easily accessible cobalt catalyst for selective hydrogenation of C=O bonds. *J. Am. Chem. Soc.* **137**, 7998–8001 (2015).
23. S. Rösler, M. Ertl, T. Irrgang, R. Kempe, Cobalt-catalyzed alkylation of aromatic amines by alcohols. *Angew. Chem. Int. Ed.* **54**, 15046–15050 (2015).
24. N. Deibl, R. Kempe, General and mild cobalt-catalyzed C-alkylation of unactivated amides and esters with alcohols. *J. Am. Chem. Soc.* **138**, 10786–10789 (2016).
25. F. Kallmeier, T. Irrgang, T. Dietel, R. Kempe, Highly active and selective manganese C=O bond hydrogenation catalysts: The importance of the multidentate ligand, the ancillary ligands, and the oxidation state. *Angew. Chem. Int. Ed.* **55**, 11806–11809 (2016).
26. N. Deibl, R. Kempe, Manganese-catalyzed multicomponent synthesis of pyrimidines from alcohols and amidines. *Angew. Chem. Int. Ed.* **56**, 1663–1666 (2017).
27. F. Kallmeier, B. Dudziec, T. Irrgang, R. Kempe, Manganese-catalyzed sustainable synthesis of pyrroles from alcohols and amino alcohols. *Angew. Chem. Int. Ed.* **56**, 7261–7265 (2017).
28. G. Zhang, T. Irrgang, T. Dietel, F. Kallmeier, R. Kempe, Manganese-catalyzed dehydrogenative alkylation or α-Olefination of alkyl-substituted N-heteroarenes with alcohols. *Angew. Chem. Int. Ed.* **57**, 9131–9135 (2018).
29. D. Forberg, T. Schwob, M. Zaheer, M. Friedrich, N. Miyajima, R. Kempe, Single-catalyst high-weight% hydrogen storage in an *N*-heterocycle synthesized from lignin hydrogenolysis products and ammonia. *Nat. Commun.* **7**, 13201 (2016).
30. D. Forberg, T. Schwob, R. Kempe, Catalytic condensation for the formation of polycyclic heteroaromatic compounds. *Nat. Commun.* **9**, 1751 (2018).
31. T. Schwob, R. Kempe, A reusable Co catalyst for the selective hydrogenation of functionalized nitroarenes and the direct synthesis of imines and benzimidazoles from nitroarenes and aldehydes. *Angew. Chem. Int. Ed.* **55**, 15175–15179 (2016).
32. J. Pritchard, G. A. Filonenko, R. van Putten, E. M. J. Hensen, E. A. Pidko, Heterogeneous and homogeneous catalysis for the hydrogenation of carboxylic acid derivatives: History, advances and future directions. *Chem. Soc. Rev.* **44**, 3808–3833 (2015).
33. X.-J. Dai, C.-J. Li, En route to a practical primary alcohol deoxygenation. *J. Am. Chem. Soc.* **138**, 5433–5440 (2016).
34. G.-H. Wang, J. Hilgert, F. H. Richter, F. Wang, H.-J. Bongard, B. Spliethoff, C. Weidenthaler, F. Schüth, Platinum–cobalt bimetallic nanoparticles in hollow carbon nanospheres for hydrogenolysis of 5-hydroxymethylfurfural. *Nat. Mater.* **13**, 293–300 (2014).
35. M. J. Climent, A. Corma, S. Iborra, Conversion of biomass platform molecules into fuel additives and liquid hydrocarbon fuels. *Green Chem.* **16**, 516–547 (2014).
36. D. C. Blakemore, L. Castro, I. Churcher, D. C. Rees, A. W. Thomas, D. M. Wilson, A. Wood, Organic synthesis provides opportunities to transform drug discovery. *Nat. Chem.* **10**, 383–394 (2018).
37. B. Morandi, B. Mariampillai, E. M. Carreira, Enantioselective cobalt-catalyzed preparation of trifluoromethyl-substituted cyclopropanes. *Angew. Chem. Int. Ed.* **50**, 1101–1104 (2011).
38. S.-B. Yang, F.-F. Gan, G.-J. Chen, P.-F. Xu, An efficient one-pot synthesis of ω-hydroxy ketones from lactones. *Synlett* **16**, 2532–2534 (2008).
39. E. Bêche, P. Charvin, D. Perarnau, S. Abanades, G. Flamant, Ce 3d XPS investigation of cerium oxides and mixed cerium oxide ($Ce_xTi_yO_z$). *Surf. Interface Anal.* **40**, 264–267 (2008).
40. Y. Lykhach, S. M. Kozlov, T. Skála, A. Tovt, V. Stetsovych, N. Tsud, F. Dvořák, V. Johánek, A. Neitzel, J. Myslivečeк, S. Fabris, V. Matolín, K. M. Neymann, J. Libuda, Counting electrons on supported nanoparticles. *Nat. Mater.* **15**, 284–288 (2016).

Acknowledgments: We thank E. Arzt for his support through the INM. We also thank A. Gollwitzer and T. Dietel for the x-ray characterization of complex **I**, J. Schmauch for assistance with the EELS measurements, and O. Lytken for support regarding the XPS analysis. **Funding:** We acknowledge the financial support from the Deutsche Forschungsgemeinschaft, KE 756/21-2. **Author contributions:** T.S. carried out the synthesis of the catalyst, the catalyst

characterization, and the catalytic reactions. P.K. and N.d.J. performed the HAADF-STEM, EDX, and EELS analyses. C.P. and H.-P.S. accomplished the XPS analysis. T.S. and R.K. designed the experiments and co-wrote the manuscript. **Competing interests:** The authors declare that they have no competing interests. **Data and materials availability:** Crystallographic data CCDC 1865045 contains the supplementary crystallographic data for this paper and can be obtained free of charge from The Cambridge Crystallographic Data Centre. All data needed to evaluate the conclusions in the paper are present in the paper and/or the Supplementary Materials. Additional data related to this paper may be requested from the authors.

Submitted 10 September 2018
Accepted 17 September 2019
Published 15 November 2019
10.1126/sciadv.aav3680

Citation: T. Schwob, P. Kunnas, N. de Jonge, C. Papp, H.-P. Steinrück, R. Kempe, General and selective deoxygenation by hydrogen using a reusable earth-abundant metal catalyst. *Sci. Adv.* **5**, eaav3680 (2019).

Science Advances

General and selective deoxygenation by hydrogen using a reusable earth-abundant metal catalyst

T. Schwob, P. Kunnas, N. de Jonge, C. Papp, H.-P. Steinrück and R. Kempe

Sci Adv **5** (11), eaav3680.
DOI: 10.1126/sciadv.aav3680